
White Dwarfs in Globular Clusters

S. Moehler¹ and G. Bono^{1,2,3}

¹ European Southern Observatory, Karl-Schwarzschild-Str. 2, 85748 Garching, Germany, smoehler@eso.org

² Dept. of Physics, Univ. of Rome Tor Vergata, via della Ricerca Scientifica 1, 00133 Rome, Italy, bono@roma2.infn.it

³ INAF-Osservatorio Astronomico di Roma, via Frascati 33, 00040 Monte Porzio Catone, Italy

We review empirical and theoretical findings concerning white dwarfs in Galactic globular clusters. Since their detection is a critical issue we describe in detail the various efforts to find white dwarfs in globular clusters. We then outline the advantages of using cluster white dwarfs to investigate the formation and evolution of white dwarfs and concentrate on evolutionary channels that appear to be unique to globular clusters. We also discuss the usefulness of globular cluster white dwarfs to provide independent information on the distances and ages of globular clusters, information that is very important far beyond the immediate field of white dwarf research. Finally, we mention possible future avenues concerning globular cluster white dwarfs, like the study of strange quark matter or plasma neutrinos.

1 Introduction

During the last few years white dwarfs have been the topic of several thorough review papers focused on rather different aspects. The interested reader is referred to [85] and to [86] for a comprehensive discussion concerning the use of white dwarfs as stellar tracers of Galactic stellar populations and the physics of cool white dwarfs. The advanced evolutionary phases and their impact on the dynamical evolution of open and globular clusters have been reviewed by [116], while [4] provide a comprehensive discussion of the use of white dwarfs to constrain stellar and cosmological parameters together with a detailed analysis of the physical mechanisms driving their evolutionary and pulsation properties.

The advantages of using cluster white dwarfs over field white dwarfs in studying the formation, physical properties, and evolution of these stars come from a number of properties of star clusters. *i)* – White dwarfs in globular or open clusters are located at the same distance and have (in general) the

same reddening. Moreover and even more importantly, when moving from hot to cool white dwarfs the colours of cluster white dwarfs are systematically bluer than those of main sequence stars (see Fig. 1). This means that to properly identify cluster white dwarfs we can use the colour-magnitude diagram instead of a colour-colour plane. Therefore, the identification of cool cluster white dwarfs is not hampered by the thorny problem of colour degeneracy with main sequence stars that affects field white dwarfs ([85]). *ii*) – For cluster white dwarfs we can trace back the evolutionary properties of the progenitors, since both the chemical composition and the typical mass at the turn-off of the cluster are well-known. While there is some evidence that the most massive globular clusters (e.g. ω Cen, NGC 1851, NGC 2808, NGC 6388, NGC 6441) probably have a more complicated star formation and chemical enrichment history, most globular clusters are essentially mono-metallic systems with respect to iron with a negligible spread in age. This provides the opportunity to constrain the initial-to-final mass relation of white dwarfs and to improve the knowledge of the physical mechanisms governing their final fate ([86]; [114]). *iii*) – According to current evolutionary predictions the number of white dwarfs in a globular cluster with an age of 12 Gyr and a Salpeter-like initial mass function ($\alpha = 2.35$) is about a factor of 300 larger than the number of horizontal branch stars ([33]). This means that the expected local density of white dwarfs in a globular cluster is several orders of magnitude larger than the local densities of the halo, thick disk, and thin disk white dwarf populations, thus allowing us to observe large homogeneous samples of white dwarfs without the need for wide-field surveys.

The main drawback for white dwarfs located in globular clusters is that they are faint objects severely affected by crowding problems. Photometric observations are well possible with the Hubble Space Telescope (HST) and profit from software packages that allow astronomers to obtain precise measurements even in crowded fields. Spectroscopy, however, poses a different problem: HST is a too small telescope and lacks the multiplexing capacities that enable efficient observations in globular clusters. The disentangling of overlapping spectra in ground based observations is a rather difficult process, as the contributions from the different stars vary strongly with wavelength. Early spectroscopic investigations (e.g. [145]; [148]) were hampered by the fact that their targets were selected from HST photometry, which had usually been observed rather close to the cluster cores. Good photometry of the outer regions of globular clusters facilitate spectroscopic observations enormously, as the problem of background subtraction is immensely reduced if there are no bright stars close to the white dwarfs (e.g. [56]).

In a recent investigation [55] called attention to the evidence that the radial distribution of young white dwarfs in NGC 6397 is significantly more extended than the radial distribution of both older white dwarfs and the most massive main sequence stars. To account for this peculiar trend they suggest that the white dwarfs in this cluster do not experience a quiescent birth, but they receive a natal kick. This scenario has been suggested originally by [70] and

received additional support from the theoretical investigations of [94, 95, 96]. In particular, he found that asymmetric winds on the asymptotic giant branch can generate a kick affecting the trajectory of the resulting white dwarfs. This mechanism would explain why young white dwarfs are less centrally concentrated than their progenitors. The radial distribution of young white dwarfs in ω Cen observed by [38] provides some support for that scenario.

The impact that energetic white dwarfs (i.e. the young white dwarfs affected by the velocity kick) have on the structural properties of the host cluster has been investigated by [97]. They found that the white dwarf kicks lose a significant fraction of their energy in the central region of the cluster. This means that these objects can either delay the core collapse or increase the size of the cluster cores. These predictions were soundly confirmed by [76] using a Monte Carlo cluster evolution code. They found that for globular clusters with velocity dispersions similar to the kick speed, the white dwarfs' kicks can delay the phase of core contraction and increase by one order of magnitude the current ratio between the core and the half-mass radius.

If this kick effect is indeed present in other globular clusters as well, it will be very helpful for the study of white dwarfs in globular clusters, as it would put the youngest (and therefore brightest) white dwarfs into the less crowded outer regions.

Beyond the obvious observational complications, we still lack a detailed understanding of the impact of the high density environment of globular clusters on the formation and evolution of cluster white dwarfs ([149]).

As the exploration of white dwarfs in globular clusters is an extremely active and rapidly growing field we want to state here that this review contains information from papers or preprints (accepted for publication) available by December 2010.

2 Searches and Detections

As already mentioned above, white dwarfs in globular clusters are not the most easily observable stars. Their direct detection is hampered by the severe crowding problems in observations deep enough to locate white dwarfs, which explains why it took so long to really identify the first white dwarfs in a globular cluster.

2.1 Direct Identification

The pioneering ground-based photometric investigations concerning white dwarfs in globular clusters date back to the late 1980's ([153] – ω Cen; [169] – M 71). However, detailed investigations of globular cluster white dwarfs were undertaken only after the refurbishment of the HST with its Wide Field and Planetary Camera 2 (**WFPC2**). Several candidate white dwarfs were then soon identified in quite a few globular clusters. One should keep in mind that

the masses assigned to white dwarf sequences in globular clusters are based on comparisons with theoretical tracks and therefore strongly depend on the assumed distance modulus and reddening of the respective cluster. The clusters are listed by the date of the first discovery paper.

NGC 5139 (ω Cen) – This is the most massive Galactic globular cluster and it is therefore not surprising that the search for white dwarfs dates back to [153], who detected two dozen white dwarf candidates using photometry observed with the Faint Object Spectrograph and Camera 1 at the ESO 3.6m telescope, and to [67], who detected four white dwarf candidates using WFPC2 data. More recently, [149] detected more than 2,000 white dwarf candidates in three out of the nine pointings observed with the Advanced Camera for Surveys (**ACS**) on board the HST, which were located across the cluster center. Moreover, deep H_α measurements support the evidence that about 80% of these cluster white dwarfs are also H_α -bright. In order to account for this empirical evidence [149] suggested that a fraction of the white dwarf candidates might be He-core white dwarfs, and therefore the aftermath of a violent mass loss event (see end of Sect. 4.2 for more details). Interestingly enough, [37] also noted that candidate He-core white dwarfs have been identified in stellar clusters showing evidence for extreme mass loss on the red giant branch, like the metal-rich old open cluster NGC 6791 (presence of extreme horizontal branch stars) and the globular clusters ω Cen and NGC 2808 (presence of late hot helium flashers, cf. Sect. 4.2). Such extreme mass loss could in turn also yield stars that avoid the He-core flash completely and thus become He-core white dwarfs.

NGC 6838 (M71) – On the basis of deep multi-band data observed with the Canada-France-Hawaii Telescope [169] detected a dozen white dwarfs in this metal-rich globular cluster. By adopting an apparent distance modulus of $(m - M)_V = 13.70$ they argued that the cluster white dwarf sequence was either too faint or too blue when compared to DA field white dwarfs, but in plausible agreement either with DB field white dwarfs or with a sequence of DA white dwarfs about $0.1 M_\odot$ more massive than typical DA white dwarfs in the Galactic disk. The small number of objects and the shallow depth of the colour-magnitude diagram puts these conclusions on somewhat weak footing and deeper observations would be very helpful. Moreover, they identified a parallel sequence of blue objects, located between the white dwarf sequence and the main sequence, which they identified as a sequence of cluster cataclysmic variables.

NGC 6397 – By using deep WFPC2 observations [155] first detected a candidate white dwarf sequence in NGC 6397, which showed good agreement with theoretical predictions for white dwarfs with a mass of $0.5 M_\odot$ (assuming an apparent distance modulus of $(m - M)_I = 12.2$) for stars brighter than $m_{814} \approx 24.5$. At fainter magnitudes the observed numbers exceeded the predicted ones, probably due to contamination by,

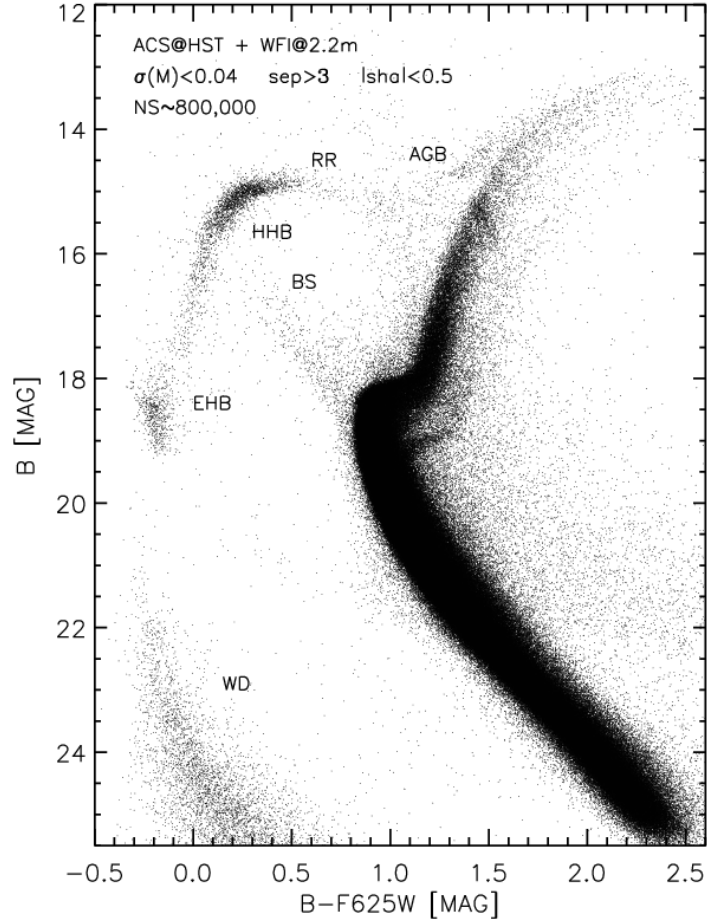


Fig. 1. Composite $B, B-F625W$ colour-magnitude diagram of ω Cen based on data collected with the ACS and with the Wide Field Imager (WFI) available at the 2.2m ESO/MPG telescope ([44]; [37]). The final catalog includes 1.7 million stars. The stars plotted in this diagram were selected according to *sharpness*, *separation* and intrinsic photometric error (see labeled values). From top to bottom the labels mark specific evolutionary phases: the Asymptotic Giant Branch (**AGB**), the RR Lyrae instability strip (RR), the Hot Horizontal Branch (HHB), the Blue Stragglers (BS), the Extreme Horizontal Branch (EHB, including hot helium flashers, see Sec. 4.2), and the White Dwarf (WD) cooling sequence.

e.g., background galaxies. Independent observations of the same cluster with WFPC2 were collected by [49]. They also detected the white dwarf sequence, which they fit with models for $M_{\text{WD}} = 0.55 \pm 0.05 M_{\odot}$ with an intrinsic dispersion below $0.05 M_{\odot}$ (for a true distance modulus $(m - M)_0 = 11.9$ and a reddening of $E_{B-V} = 0.18$). This comparison illustrates the uncertainties associated with a straightforward fitting of observed white dwarf sequences with theoretical models. Using deep ACS photometry (down to $m_{F814W} = 28$) of NGC 6397 [89] detected securely for the first time in a globular cluster the blueward turn of the white dwarf sequence expected due to collisionally induced absorption (**CIA**) by H_2 in H-rich white dwarf atmospheres. In their paper they also provide a very good discussion of the various parameters affecting a fit of the white dwarf cooling curve with theoretical models.

In 1998 [50] detected seven centrally concentrated UV-bright objects in WFPC2 observations together with the bright end of the white dwarf cooling sequence. Three of the UV-bright objects had been previously identified as cataclysmic variables. While a fourth one is also a probable cataclysmic variable candidate, the remaining three show no evidence for variability (so-called “Non-Flickerers”) and are good candidates for He-core white dwarfs. In 2001 [194] found three additional “Non-Flickerers” from WFPC2 observations. These “Non-Flickerers” form a sequence parallel to the main white dwarf sequence, but brighter by about 2 magnitudes in V_{555} . The fainter “Non-Flickerers” ($V_{555} \approx 23$) show strong H_{α} absorption ($H_{\alpha} - R_{675} > 0.5$). The “Non-Flickerers” are significantly more centrally concentrated than the main sequence stars. Since mass segregation in globular clusters causes the more massive stars to sink towards the center, this argues for fairly massive companions, if these objects are indeed He-core white dwarfs. Due to the observed blue broad-band colours, which rule out all but the lowest mass main sequence stars (cf. Sect. 4.1), the most probable companions are white dwarfs.

NGC 6121 (M 4) – Using WFPC2 data [170] found a well defined white dwarf sequence, which is again in agreement with a mean mass of the white dwarfs of $0.5 M_{\odot}$ for an assumed distance modulus $(m - M)_V = 12.65$ (note that this is close to the best-fit distance of $(m - M)_V = 12.57$ derived by [87]) and an intrinsic dispersion below $0.05 M_{\odot}$. Here the observed number of white dwarf candidates lies below theoretical predictions at fainter magnitudes, possibly due to uncertainties in the completeness corrections, to non-DA contributions and/or to incorrect assumptions concerning the C/O core compositions of the white dwarfs. Subsequent deeper observations collected with the same instrument allowed [173] and [83] to trace the white dwarf sequence down to $m_{606W} \approx 30$, which they used to derive an age for the cluster (see Sect. 5.2).

NGC 104 (47 Tuc) – By using the Faint Object Camera on board the HST [156] found 9 objects in the white dwarf region of the colour-magnitude diagram. In 2001 [214] detected the white dwarf sequence in WFPC2

observations down to $m_{555} \approx 27$ and used it to determine the age and the distance of this cluster (see Sects. 5.2 and 5.1, respectively). UV observations with WFPC2 by [71] show a sequence of 12 hot white dwarf candidates (in agreement with theoretical expectations) as well as a large number of objects between the blue straggler and the white dwarf sequence. Unfortunately, [214] and [71] were published within a few months of each other so that the authors could not compare their results. The search for cluster white dwarfs in 47 Tuc has been hampered by the fact that this cluster is projected onto the wing of the Small Magellanic Cloud ([214]). However, by adopting both far-UV (**FUV**) images collected with the Space Telescope Imaging Spectrograph (**STIS**) on board the HST and F336W images collected with WFPC2 [123] detected a well defined white dwarf sequence in the center of the cluster. Thanks to the strong temperature sensitivity of the FUV-optical colour they also identified a sequence of candidate cataclysmic variables (16) located between the white dwarf and the main sequence stars. According to theoretical and statistical arguments they estimate that at least a half of these objects should belong to the cluster.

NGC 6752 – Data collected with WFPC2 allowed [168] to identify the white dwarf cooling sequence and to determine the distance of the globular cluster (see Sect. 5.1).

NGC 2808 – Near-UV (**NUV**) and FUV STIS observations of NGC 2808 ([61], see also [34]) reveal a population of candidate hot white dwarfs (22 objects brighter than $m_{NUV} \approx 21$) and also a number of cataclysmic variable candidates lying between the white dwarf and the main sequence in the UV colour-magnitude diagram (about 50 objects, two of which are variable).

NGC 7078 (M15)– A clear identification of cluster white dwarfs was recently provided by [62] using deep FUV and NUV ACS images. In particular, they identified 28 white dwarfs and ≈ 60 candidates for cataclysmic variables. These findings appear very promising, since M15 is a very metal-poor ($[\text{Fe}/\text{H}] = -2.26$, [90]) globular cluster characterized by a very dense core ($\rho_c = 7 \times 10^6 M_\odot pc^{-3}$, [199]) and a very high central velocity dispersion [65]. In order to account for these features the presence of an intermediate mass black hole ([77]) or a high mass concentration caused by mass segregation of neutron stars and massive white dwarfs ([9]) have been suggested.

NGC 6093 (M80) – Two dozens of candidate white dwarfs have been recently identified by [63] in M80 using FUV and NUV ACS images.

NGC 3201 – A dozen of bright candidate white dwarfs have also been recently identified by [31] in NGC 3201 using deep V,I-band ACS images at a limiting magnitude of $V \approx I \approx 24.5$ mag.

In summary, observations of white dwarfs in globular clusters indicate that the cooling sequences in general agree with theoretical expectations. Unusual

populations observed in other regions of the colour-magnitude diagram (most notably along the horizontal branch), however, also affect the white dwarf cooling sequence (e.g. the He-core white dwarf candidates in ω Cen, see beginning of this section, and NGC 6791, see Sect. 4.2).

2.2 Indirect Identification

So far we discussed the identification of white dwarfs in globular clusters by looking for their cooling sequence in the colour-magnitude diagrams. The detection of white dwarfs in binary systems in the clusters requires rather different methods. As the section below will show, however, ignoring them would severely bias our knowledge about white dwarfs in globular clusters.

Current theoretical predictions accounting for dynamical and evolutionary processes suggest that the binary fraction in dense globular clusters, with ages ranging from 10 to 14 Gyr, is of the order of 10% ([104]; [54]; [101]; [73]). However, theoretical predictions concerning the evolution with time of the binary fraction in globular clusters are not very well established yet. Predictions based on full N-body simulations and including binary stellar evolution indicate that the binary fraction in the cluster core increases with time ([101]). On the other hand, predictions based on a simplified dynamical model and accounting for binary stellar evolution suggest that the binary fraction in clusters decreases with time ([104]). The two different approaches to account for the fraction of binary stars detected in globular clusters require a modest and a large fraction of primordial binaries, and in turn different collisional rates. The reason for this discrepancy is not clear, but it has been suggested that the above difference is mainly due to differences in the adopted initial conditions and physical assumptions ([72]).

On the other hand, empirical evidence based on continuous photometric monitoring (8.3 days) with WFPC2 of some 46,000 main sequence stars in 47 Tuc indicates that the overall binary frequency is about $14 \pm 4\%$ ([1]). This estimate accounts for detached eclipsing binaries and for contact binaries and might still be a lower limit. From the overluminous white dwarfs in M4 [87] estimate a binary fraction among the white dwarfs of 0.11 ± 0.05 , in agreement with the percentage of hard binaries among field white dwarfs (soft binaries would be destroyed in M4). By using the colour distribution of main sequence stars, based on deep ACS images for 13 low-density globular clusters, [192] found that the current minimum fraction of binary stars is of the order of 6% inside the core radius, while the global fraction ranges from 10% to 50%. According to the above numbers it is not surprising that globular clusters should host a broad range of exotic objects that show up as faint X-Ray sources. Of those, the following have been identified in globular clusters so far: low-mass X-Ray binaries (a neutron star accreting from a companion) and their progeny, the millisecond pulsars; chromospherically or magnetically active binaries (two main sequence stars or a main sequence star and an evolved companion); and cataclysmic variables (a white dwarf

accreting from a low-mass companion). The formation rate of these objects in globular clusters is expected to be orders of magnitude higher than in the Galactic disk ([118]; [47]). The advent of the *Chandra* X-Ray Observatory and of HST provided the opportunity to investigate these objects in the central regions of globular clusters (see [203] for an extensive review of X-ray sources in globular clusters). The cataclysmic variables appear to be the progeny of either primordial binaries or stellar encounters and they have been identified in several globular clusters. In particular, *Chandra* X-ray observations in combination with HST photometry identified nine cataclysmic variables in NGC 6397 ([194]), 22 in 47 Tuc ([92]; [93]), and two (possibly three) in M 4 ([8]). Additional optical counterparts of faint *Chandra* X-ray sources in the post core collapsed globular cluster NGC 6397 have been recently provided by [48]. They identified more than a dozen cataclysmic variables and found that they split into two groups: the brighter one in which the optical emission is dominated either by the companion or by the accretion disk and the fainter one in which the optical emission is dominated by the white dwarf. They also found that the former group is more centrally concentrated than the latter one and suggested that the difference might be caused by an evolutionary process. The cataclysmic variables are formed in the very innermost regions of the globular cluster by dynamical interaction and are then scattered to larger distances as they age. Using FUV STIS spectra [125] identified four dozens of stellar exotica in 47 Tuc. They found that the number of observed cataclysmic variables agrees with the predicted one within a factor of 2–3.

Optical and FUV data collected with HST and covering long time intervals (several years) also provided the opportunity to identify outbursting cataclysmic variables in a few globular clusters ([185], [186]). This approach is very useful to unambiguously identify cluster cataclysmic variables, since the spectroscopic follow-up of candidates located in the crowded central regions is difficult ([124]).

On the basis of these X-ray and optical surveys of a dozen globular clusters a remarkable correlation has been found between the stellar encounter rate and the number of X-ray sources in the cores of globular clusters ([163]).

Contrary to expectations, simulations by [187] showed that the production rate of cataclysmic variables in globular clusters is comparable to that observed in the field. Due to the high density environment in globular clusters, however, hard binaries dominate there, which have a faster evolution. Moreover, the simulations also predict a new class of cataclysmic variables that are formed by exchange interactions, i.e. without a common envelope phase. Such cataclysmic variables are formed preferably with donor masses on the main sequence of more than $0.7 M_{\odot}$ and are short-lived when compared to classical field cataclysmic variables. These generally shorter lifetimes for globular cluster cataclysmic variables imply a reduction in their expected number, at any given time, by roughly a factor of three. Another interesting prediction of these simulations is that the canonical 2–3 hours period gap observed among

field cataclysmic variables should be smeared out in the dynamically formed globular cluster cataclysmic variables.

Numerical simulations by [105] accounting for binary formation via physical collisions (based on smoothed particle hydrodynamics) and for the metallicity dependence in the formation and evolution of close binaries also predict that the formation rate of cataclysmic variables and AM CVn systems (white dwarf binaries with one of the two white dwarfs undergoing a Roche lobe overflow) in the field and over the entire cluster are very similar. There is, however, a larger variety of formation channels for binaries in globular clusters than for their field counterparts: primordial binaries, post-exchange binaries, and physical collisions between main sequence and red giant stars.

Ultraluminous X-ray sources have X-Ray luminosities well above the Eddington limit for a neutron star accreting helium and it has been suggested that these systems might harbor a black hole (BH) X-ray binary ([7]; [32]). Such X-ray sources have been recently identified in a Galactic globular cluster (NGC 4472, [139]) and in globular clusters belonging to external galaxies ([121]; [107]). Their X-Ray properties suggest that these systems might consist of a stellar-mass black hole and a compact donor (i.e. they are black hole–white dwarf binaries). The formation rates of such system in globular clusters was investigated by [106]. They accounted for binary exchange and physical collisions and found that the only possibility to form black hole–white dwarf binaries is via hardening and/or the formation of a triple system. Moreover, they suggest that in order to explain the empirical evidence with black hole–white dwarf binaries between 1% and 10% of the black holes present in the core of a globular cluster should interact with the stellar population located inside the cluster core.

3 Spectral Types

Photometric observations alone are generally not sufficient to distinguish DA from non-DA stars, although H-rich DAs and He-rich DBs in principle can be distinguished by their photometric properties alone in the temperature range $10,000\text{ K} \leq T_{\text{eff}} \leq 15,000\text{ K}$ (see [23]). Based on this method [168] classified two white dwarfs in NGC 6752 as DBs. However, without a spectroscopic confirmation, those two stars can also be explained as high-mass DA white dwarfs, possibly a product of merging. Also the brightest white dwarf in M 4 ($V=22.08$) might be a hot (27,000K) DB star ([171]). In 1999 [66] showed a spectrum observed with the Faint Object Spectrograph (**FOS**) on board the HST covering the H_{β} region of a “Non-Flickerer” in NGC 6397, which clearly showed that the spectrum was H-rich. In 2000 [145] published the first ground-based spectra of four white dwarfs in a globular cluster (NGC 6397) observed with the FOcal Reducer/low dispersion Spectrograph 1 (**FORS1**) at the ESO-VLT, which covered the range from 3800 \AA to more than 5000 \AA . All stars were DA white dwarfs. Investigating the ratio between DA and non-

DA white dwarfs for effective temperatures ranging from 10,000 to 14,000 K in NGC 6397 [195] found that only 1, probably 4, out of sample of 126 C/O white dwarfs are of the non-DA type. Detailed analysis for field white dwarfs [197], however, indicates that the ratio between the two different samples is 4:1 for stars between 10,000 K and 15,000 K.

Later [148] also showed FORS1 spectra of five white dwarfs in NGC 6752, all of which were once again H-rich.

In 2005 [112] showed spectra of 21 white dwarfs in the young (650 Myr) open cluster NGC 2099 (>30% of the known white dwarfs in that cluster) observed with the Gemini Multi-Object Spectrograph at the Gemini telescope and with the Low-Resolution Imaging Spectrometer (**LRIS**) at the Keck telescope, none of which was He-rich. Cluster members have estimated effective temperatures between 13,000 K and 18,000 K in the observed magnitude range. Allowing for 4–5 contaminating field stars, one would expect to find 4 DBs from the 4:1 DA:non-DA ratio observed among field white dwarfs of similar temperatures ([180], [197]). It was noted by [10] that the mass distribution of field DB stars lacks the high-mass tail observed for DA white dwarfs. Newer observations by [205], on the other hand, find no difference in the mass distribution between DB and DA stars. Spectroscopic analyses by [111] yield rather high masses of up to $1.1 M_{\odot}$ for the bright white dwarfs in NGC 2099, consistent with the youth of that cluster. Several explanations for the possible lack of DB stars among massive white dwarfs were discussed by [112]: *i*) – More massive white dwarfs have thicker hydrogen layers, which may prevent the formation of a convection zone mixing helium to the hydrogen layer. Such a convection zone has been suggested to cause the appearance of DB stars at about 30,000 K ([134]; [85])). This explanation, however, has no quantitative support so far and the currently assumed hydrogen layers are much thicker than those assumed by [134]. *ii*) – The removal efficiency for the hydrogen layer depends on mass. *iii*) – Binary evolution may result preferably in DA white dwarfs (in binary systems and also as single stars, [136]).

Also LRIS spectroscopy of white dwarfs in NGC 6791 by [113], showed only H-rich spectra for all nine targets with sufficient S/N.

The situation changed recently, when [209] and [114], both using LRIS at Keck, detected DB type white dwarfs in the open clusters NGC 6633 (0.5 Gyr) and NGC 6819 (1.5 Gyr), respectively.

Observations of 19 probable cluster white dwarfs in M 4 by [56] show all stars to be H-rich, whereas 4–5 He-rich ones would have been expected (assuming a ratio of 4.2:1). Combining their data with results for other globular and open clusters (for a total of 140 white dwarfs) the authors derive a probability of $6 \cdot 10^{-9}$ that the DA:non-DA rate in clusters is the same as in the field. Due to the large range in mass, age, and metallicity covered by the sample the authors rule out these parameters as possible explanations. Suppression of the formation of non-DA stars by the density in the clusters is ruled as the required density is above that of most globular clusters and far above any

open cluster. Transforming a non-DA into a DA via accretion is also ruled out. The finding therefore remains unexplained for now.

4 White Dwarf Formation and Evolution

The minimum mass value for carbon ignition in the core is the so-called M_{up} , while M_{mas} defines the minimum mass value to ignite neon at the center. Stellar structures with initial masses smaller than M_{up} produce degenerate C/O cores during the asymptotic giant branch phase. Current evolutionary prescriptions ([26]; [140]; [80]; [157]) suggest that these stars finish their evolution either as C/O white dwarfs (efficient mass loss along the asymptotic giant branch) or with a carbon deflagration ([102]; [98]) if the mass of the C/O core becomes larger than the Chandrasekhar mass (mild mass loss along the asymptotic giant branch). Stellar structures with initial masses larger than M_{mas} experience all the nuclear burning stages and finish their evolution as iron core collapse supernovae ([213]; [137]). Stellar structures with initial masses between M_{up} and M_{mas} , the so-called super-AGB stars, start to ignite carbon in a partially degenerate off-center shell. After a few shell flashes these structures eventually start to burn carbon in the center and finish their evolution either as massive O/Ne white dwarfs ([151]; [196]; [78]; [188]) or as electron-capture supernovae where the core collapse is triggered by electron captures before the neon ignition ([207]). Evolutionary calculations indicate that the value of M_{up} strongly depends on the assumptions adopted to deal with semi-convection and convective overshooting. By using three evolutionary codes with different mixing algorithms, [162] found that, at fixed metal abundance, the value of M_{up} ranges from 7.5 to 9.0 M_{\odot} .

White dwarfs in globular clusters thus have a broad range of progenitor masses, but they are currently produced by progenitors with stellar masses of about 0.8-1.0 M_{\odot} ([172]). Due to their long cooling times massive white dwarfs in globular clusters will generally be extremely faint. However, massive cluster white dwarfs may currently evolve from blue stragglers or from the merging of close white dwarf binaries (see, e.g., [142]). The general evolutionary properties of white dwarfs have been investigated in many papers (see, e.g., [126]; [51]; [22]; [3]; [184]; [75]; and references therein). New cooling sequences for white dwarfs by [182] take into account accurate boundary conditions, which are based on model atmospheres and on C/O chemical abundance profiles (based in turn on detailed evolutionary calculations from the BASTI data base). The authors also analysed in detail the impact of the input physics (mixing during central H and He burning phases, number of thermal pulses, progenitor metallicity, $^{12}\text{C}(\alpha, \gamma)^{16}\text{O}$ reaction rate) on the accuracy of the predicted cooling times. They found that the leading factors are the treatment of the convection during the final phases of He burning and the $^{12}\text{C}(\alpha, \gamma)^{16}\text{O}$ reaction rate.

The physical mechanisms driving the crystallization of white dwarfs has been investigated recently by [210]. They compare theoretical predictions with the colour-magnitude diagram and luminosity function of cluster white dwarfs in NGC 6397 ([89]; [176]). They found that the crystallization is a first-order phase transition and releases latent heat during this process as originally suggested by [200]. They also found that the melting temperature of white dwarf cores approaching the peak of the luminosity function is close to that of pure carbon. Moreover, they mention that the comparison between predicted and empirical white dwarfs cooling sequences can be adopted to constrain not only the ratio between coulomb and thermal energy close to onset of crystallization, but also the C/O ratio in the center and the energy released by crystallization due to the phase separation of carbon and oxygen.

Using molecular dynamics simulations accounting for both liquid and solid phases [100] investigated the phase diagram for C/O white dwarfs. Based on the results of [210] concerning the melting temperature of white dwarf cores they predict the abundance of oxygen in these structures to be less than 60%. This evidence together with predictions concerning the treatment of convection in evolutionary models ([179]) can be adopted to constrain the effective astrophysical S factor of the $^{12}\text{C}(\alpha,\gamma)^{16}\text{O}$ nuclear reaction.

In the following subsections we briefly discuss the formation of *low-mass white dwarfs* from binary evolution and otherwise.

4.1 Binary Evolution

Empirical evidence based on field white dwarfs, for which spectroscopic mass estimates are available, indicates that only a fraction of the order of 10% has masses below $0.45 M_{\odot}$, which is the limiting mass required to remove the electronic degeneracy and to ignite He-core burning via the He-core flash ([43]). These He-core white dwarfs are generally considered to be the aftermath of binary star evolution, since single stars with such low masses are not expected to evolve to the white dwarf cooling sequence within a Hubble time. These objects underwent an episode of extreme mass loss, possibly caused by stellar encounters or by evolution in compact binaries, while they approach the tip of the red giant branch (**RGB**, [122]).

In 2003 [84] published a study on the effects of binary evolution on the white dwarfs in globular clusters. Binary formation by exchange interactions between hard binaries and single stars in globular clusters promotes the production of He-core white dwarfs as it increases the average secondary mass in binaries containing C/O white dwarfs or neutron stars (thereby increasing the probability of mass transfer episodes). In addition the final He-core white dwarf will be removed preferably from these systems during ensuing exchange interactions. Tidal captures followed by mergers or direct stellar collisions involving red giants result in binaries with a red giant core (= proto He-core white dwarf) and a more massive companion, which accreted most of the red giant's envelope (unless that was ejected). Low-mass He-core white dwarfs are,

at fixed effective temperature, brighter than typical C/O-core white dwarfs and the cooling times of the former objects are significantly longer than the latter ones. This means that even a small fraction of He-core white dwarfs significantly increases the number of observed bright white dwarfs in globular clusters ([42]; [43], see also Sect. 2.1 for ω Cen and Sect 4.2 for NGC 6791).

The globular cluster NGC 6397 shows a centrally concentrated population of UV-bright stars ([50]; [66]; [194]; see also Sect. 2.2). Spectroscopic follow-up collected with the FOS by [66] indicates that the observed non-variable UV bright star is a binary system consistent with a He-core white dwarf and an unseen massive companion being either a neutron star or a massive white dwarf. This was the first He-core white dwarf identified in a globular cluster. Detailed investigations by [84] assuming various values for the thickness of hydrogen layers and the companion masses (neutron stars, C/O white dwarfs) suggest that the “Non-Flickerers” in NGC 6397 are young objects with C/O white dwarf companions, whereas neutron star companions do not provide self-consistent solutions. This is in agreement with the lack of X-ray emission from “Non-Flickerers” observed by [82].

Using ACS multi-band photometry of NGC 6397 [195] found two dozen of hot objects forming a well defined sequence parallel to the canonical sequence of C/O-core white dwarfs, which are best explained by He-core white dwarfs with masses of 0.2–0.3 M_{\odot} . Moreover, these objects also show red H_{α} -R colors suggesting that they have strong H_{α} absorption lines, which excludes them from the sample of cataclysmic variables already identified in this globular cluster. These objects can only be produced by violent mass loss events (e.g. during binary evolution), which is also in agreement with their radial distribution being more centrally peaked than that of C/O white dwarfs and main sequence stars, but similar to that of the Blue Stragglers. The authors performed a detailed analysis concerning the nature and the mass of their companions and found that the companions cannot be main sequence stars, but have to be heavy C/O white dwarfs.

The position of the second He-Core white dwarf in 47 Tuc (identified from FUV spectroscopy by [125]) in the colour-magnitude diagram agrees quite well with that of candidate He-core white dwarfs recently identified in ω Cen ([37]) and in NGC 6397 ([195]). The effective temperature ($\sim 21,000$ K) and the radius ($R \sim 0.05 R_{\odot}$) derived for this object agree quite well with those found by [66] for the He-core white dwarfs in NGC 6397.

In an exhaustive review [18] discussed the theoretical models of globular cluster evolution and the dynamical interaction between single and binary stars. The author also provides a detailed analysis concerning the formation and evolution of binary systems including one or more compact objects. The observational techniques currently adopted to detect and characterize these exotic objects are also reviewed, including the possibility to detect gravitational radiation from the relativistic binaries in globular clusters with LISA.

4.2 Exotic Cases

A well defined white dwarf sequence in the old open cluster NGC 6791 was observed by [12] with ACS. The fit with C/O white dwarf models suggested an age of 2.4 Gyr, in stark contrast to the age of 8 Gyr derived from the main sequence turnoff of this cluster. The authors ruled out an incorrect distance modulus and incorrect assumptions on the mass of the hydrogen layer or the C/O ratio in the cores of the white dwarfs as possible explanations. He-core white dwarfs from binary evolution also cannot explain the observed white dwarf sequence, since such white dwarfs would have low masses and would therefore be too bright.

Prompted by these findings [88] explored further possible explanations and found that two effects can contribute to explain bright white dwarfs in NGC 6791: *i*) – Retardation of cooling by ^{22}Ne sedimentation ([24]; [60]), which would predict the peak of the white dwarf cooling sequence for C/O white dwarfs at $m_{606W} \approx 28\text{--}29$ (instead of $m_{606W} \approx 29\text{--}30$ from canonical models). *ii*) – Production of *massive* ($>0.4 M_{\odot}$) He-core white dwarfs due to extreme mass loss on the RGB. The idea of increased mass loss is supported by the existence of extreme horizontal branch stars in NGC 6791 ([117, 135, 131]). This second scenario can explain the peak in the luminosity function at $m_{606W} \approx 27.5$ for a cluster age of 8 Gyr, assuming that more than 50% of all low mass stars with main sequence masses above $1.6 M_{\odot}$ become He-core white dwarfs. Analyses of LRIS spectra of bright ($V \approx 22 \dots 24$) white dwarfs in NGC 6791 by [113] yielded masses below $0.46 M_{\odot}$ (threshold for core helium burning) for six out of nine probable cluster members, with the remaining three having masses of $0.47 M_{\odot}$, $0.48 M_{\odot}$, and $0.53 M_{\odot}$, supporting the high mass loss scenario outlined by [88]. Spitzer observations by [201], however, provide no evidence for enhanced mass loss.

Deeper observations by [13] show a problem with the identification of the brightest peak in the white dwarf luminosity function as He-core white dwarfs. In the new data the bright peak shows an extension to the blue, which is supposed to be caused by the more massive and older white dwarfs, which have smaller radii. In the case of He-core white dwarfs, however, this would require white dwarfs with masses above $0.5 M_{\odot}$, i.e. above the minimum mass for He-core burning. The new data show also a second, fainter peak for which a fit with canonical C/O white dwarfs gives an age of 6 Gyr. A possible solution to the puzzling difference with the turn-off age (8 Gyr, see their Fig. 10) would be the rotation of white dwarf progenitors. Rotation increases the minimum mass for the He-core flash by up to $0.15 M_{\odot}$ [143] while at the same time increasing the mass loss on the RGB. Current data do not allow us to verify this scenario.

The brighter peak of the white dwarf luminosity function in NGC 6791 at $m_{F606W} \approx 27.45$ might be explained if 34% of the observed white dwarf were in white dwarf+white dwarf binaries ([14]). To achieve this a binary fraction of 50% among the main sequence is required, similar to what has been derived

for M67 and consistent with the large number of interacting binaries observed in the field of NGC 6791.

Other old open clusters do not show such a discrepancy between the ages derived from the main sequence and from the white dwarf cooling sequence (NGC 2158 [16], M 67 [17]).

Motivated by the recent discoveries of probable He-core white dwarfs in open clusters (M 67, [130]; NGC 6791, [113], [201], [13] and in several globular clusters (NGC 6397, 47 Tuc, ω Cen), [6] performed an exhaustive theoretical investigation of the evolutionary properties of He-core white dwarfs with metal-rich progenitors. The key advantage of their approach is to account in a self-consistent theoretical framework for gravitational settling, chemical diffusion and residual nuclear burning. Moreover, they also use LTE atmosphere models explicitly including Ly_α -quasi molecular opacity to predict the white dwarf colors. They found that chemical diffusion at the base of the H-rich envelope affects the residual nuclear burning during the advanced phases of white dwarf evolution. In particular, white dwarf cooling sequences accounting for diffusion are mainly governed by the thermal content of the ions, while white dwarf cooling sequences neglecting diffusion show spuriously longer cooling times (several Gyr) due to residual hydrogen burning.

The aforementioned grid of white dwarfs cooling sequences was extended to more metal-poor progenitors, namely $Z=0.01$ and $Z=0.001$, by [166]. The cooling tracks have been followed to low effective temperatures (2500 K) and provide a very useful theoretical framework for white dwarfs in old stellar systems.

The same group in a subsequent investigation ([5]) addressed the energy released during the white dwarf cooling sequence with metal-rich progenitors by the processes of ^{22}Ne sedimentation and C/O phase separation upon crystallization. They found that the former process strongly delays the cooling rate at moderate luminosities, while the latter does so at low luminosities. They also investigated the impact of current uncertainties on ^{22}Ne diffusion coefficients on the cooling ages and found that their new white dwarf models solve the age discrepancy between the white dwarfs and the main sequence turn-off in NGC 6791.

A few massive globular clusters (e.g. ω Cen, NGC 2808, NGC 6441) show a population of very hot subluminoous horizontal branch stars, the so-called blue hook stars ([57]; [34]; [146]; [147]; [36]; [39]). The formation and evolution of these objects prompted a lively debate in the recent literature. In order to account for their photometric and spectroscopic properties the so-called “hot helium-flasher” scenario has been suggested ([41]; [57]; [34]; [43]). In this theoretical framework red giant stars experience a violent mass loss event, which decreases the total mass of these structures to below the limit for central helium ignition before approaching the tip of the red giant branch. The red giant stars with a mass slightly larger than this limit undergo a He-core flash at high temperatures either during their approach to the He-core white dwarf cooling sequence (early hot helium flasher, [41]; [57]) or along this sequence

(late hot helium flasher, [34]). Several evolutionary sequences for the hot-flasher scenario covering a broad range in heavy element abundances and physical assumptions are provided by [144]. They solve simultaneously for mixing and nuclear burning and account for convective transport either via a diffusive equation or via a mixing length approach. They also investigate the impact of chemical gradients and extra mixing at the edges of the convective regions, and in particular, the interplay between diffusion and mass loss. In particular, they found that element diffusion during the early He-core burning can transform a He-rich into a He-deficient atmosphere.

In 2006 [43] studied the consequences of this scenario for the white dwarf population in globular clusters. A globular cluster with a significant number of late hot helium-flashers will also produce a significant fraction of He-core white dwarfs (i.e. the red giant stars with a mass smaller than the limit for central helium ignition). At luminosities $L > 0.1 L_{\odot}$ He-core white dwarfs have a life time comparable to typical extreme horizontal branch stars. By assuming that a fraction of 20% of the stars in a globular cluster do not evolve through a He-core burning phase one expects twice as many white dwarfs with $L > 0.1 L_{\odot}$ than in the canonical case (all stars undergoing central helium burning). This scenario is supported by [183], who found a deficit of the order of 20% in the number of bright RGB stars in the globular cluster NGC 2808 from ACS and WFPC2 photometry. A few dozens of white dwarfs have already been identified in NGC 2808 by [61], but their limiting magnitude is too shallow to constrain the impact of the “missing giants”.

The analysis of FUV–NUV colour-magnitude diagrams of six massive globular clusters by [35] shows subluminescent stars at the hottest part of the horizontal branch for all clusters. Normal evolution at standard helium abundance ($Y=0.23$) can explain only the ‘normal’ blue and extreme horizontal branch stars. Normal evolution at enhanced helium abundance cannot explain the colour-magnitude diagrams without violating distance and reddening constraints from independent observations. Flash-mixed models for both helium abundances reproduce the luminosity range of the blue hook stars, but not the colour range (especially towards the red). Some clusters show almost no ‘normal’ extreme horizontal branch stars, but only blue horizontal branch and blue hook stars. Apparently a minimum globular cluster mass is needed to have blue hook stars, but the cause for that threshold remains unclear.

Using optical (B), NUV and FUV ACS data of the center of M15 [91] study the hot stars in this metal-poor, core-collapsed globular cluster. The colour-magnitude diagram suggests a small population of blue hook stars and He-core white dwarfs. It also shows objects between the blue hook and the He-core white dwarf region, although any canonical tracks pass through very quickly through this part of the colour-magnitude diagram (‘bright blue gap’). These objects cluster around the tracks for very young He-core white dwarfs with thick H envelopes in the colour-magnitude diagram and are concentrated strongly towards the cluster center, suggesting binarity. They might thus either be very young He-core white dwarfs or binaries with currently active mass

transfer (one X-ray source shows similar colours). Very approximate estimates of RGB collision rates in the cluster center suggest that those may be high enough to explain the production rates for the He-core white dwarfs. Mass transfer in close binaries cannot be ruled out, either. The formation rate derived for the C/O white dwarfs, however, is rather low compared to the rates at which stars evolve off the main sequence and the horizontal branch. The objects between the main sequence and the white dwarfs in FUV vs FUV–NUV show up on the main sequence in B, NUV–B. This might be explained by a population of detached white dwarf–main sequence binaries. Alternatively, they could be magnetic cataclysmic variables with truncated or absent accretion disks.

The existence of subpopulations enriched in helium ([150, 133, 52, 53]), which has been suggested to explain the multiple main sequences found in ω Cen ([11]) and NGC 2808 ([161]) also has consequences for the white dwarfs in these clusters. Recent dynamical simulations of a globular cluster, where the first generation of stars enriches the second generation with helium, have been performed by [64]. In the case of a top-heavy initial mass function for the first generation a large number of massive white dwarfs is predicted compared to the results for a Salpeter initial mass function. Accurate number ratios of white dwarfs vs. main sequence stars would allow the authors to verify their models.

Using deep multi-band photometry of ω Cen observed with the ACS and the Wide Field Imager at the ESO/MPG-2.2m telescope [44] found that empirical star counts of horizontal branch stars are on average larger (30%–40%) than predicted by canonical models. The possible occurrence of helium-enhanced stars cannot account for this excess. The authors suggested that the excess of horizontal branch stars might be due to “hot helium-flashers”. This working hypothesis implies that ω Cen should also host a sizable fraction of candidate He-core white dwarfs (cf. Sect. 2.1). The white dwarf cooling sequence of ω Cen was recently investigated by [37] using a mosaic of ACS images located across the center of the cluster. They identified more than 6,500 white dwarf candidates and the observed ratio between white dwarfs and main sequence stars is a factor of two larger than the ratio between the cooling time of C/O-core white dwarfs and main sequence lifetime. The possible occurrence of He-enhanced subpopulations does not solve the discrepancy, since an increase of the He content from 0.25 to 0.42 causes an increase in main sequence lifetime by only 15%. The possible occurrence of He-core white dwarfs might explain the observed discrepancy, since the cooling time of these structures is slower than for canonical C/O-core white dwarfs. Plain physical arguments indicate that the fraction of He-core white dwarfs necessary to explain the excess of white dwarfs ranges from 15% to 80% depending on their mean mass. These preliminary evidence — if supported by independent photometric and spectroscopic investigations — would imply that the fraction of He-core white dwarfs in at least some globular clusters might be significantly higher (at least a factor of five) than among field white dwarfs.

The possible occurrence of a significant fraction of He-core white dwarfs in ω Cen was independently supported by [40]. They performed a detailed comparison between extreme horizontal branch stars in the so-called “*blue clump*” region and evolutionary prescriptions and found that these stars can be explained as a mixture of hot helium flashers, stars with a He-enriched composition and stars with canonical He content. By comparing observed star ratios of H and He-burning phases with the ratio of evolutionary lifetimes the same authors found that at least 15% of extreme horizontal branch stars are missing in the colour-magnitude diagram. This evidence further supports the working hypothesis suggested by [37] that a non negligible fraction of bright RGB stars end up their evolution as He-core white dwarfs.

5 Astrophysical Use of White Dwarfs in Globular Clusters

Globular cluster white dwarfs play a crucial role not only to validate current evolutionary predictions, but also as a diagnostic to constrain the ages and distances of globular clusters.

5.1 Cluster Distance Determinations

The use of the white dwarf sequence as a standard candle for determining the distance to nearby globular clusters was suggested by [167]. The approach is similar to the traditional main sequence fitting procedure using local sub-dwarfs with known trigonometric parallaxes. The white dwarf sequence of the cluster is compared to a sequence constructed from local white dwarfs with accurate trigonometric parallaxes. While it may seem strange to use the faintest objects in a globular cluster to derive its distance, white dwarfs offer some advantages as standard candles when compared to main sequence stars: *i)* – They come in just two varieties - either H-rich (DA) or He-rich (DB) – *independent of their original metallicity* and, in both cases, their atmospheres are virtually free of metals. So, unlike in the case of main sequence fitting, one does not have to find local calibrators with the same metallicity as the globular clusters. *ii)* – White dwarfs are locally much more numerous than metal-poor main sequence stars and thus make it possible to define a better reference sample.

However, the method has its own specific problems, which are discussed in great detail in [214] and in [180]. Most of the discussion below is taken from these excellent papers. Indeed, the location of the white dwarf cooling sequence depends on:

- *The white dwarf mass*
On theoretical grounds, given the observed maximum luminosity reached on the asymptotic giant branch (AGB), the mass of currently forming

white dwarfs in globular clusters should be $0.53 \pm 0.02 M_{\odot}$ ([167]; [168]). Recent homogeneous evolutionary computations ([159]) from the pre-main sequence to the tip of the asymptotic giant branch suggest that, depending on the metallicity, progenitors with a stellar mass of $0.8 M_{\odot}$ form white dwarfs with masses ranging from $0.55 M_{\odot}$ ($Z=0.02$) to $0.575 M_{\odot}$ ($Z=0.0001$). Unfortunately, there are no local white dwarfs in this mass range with directly determined masses (i.e. without using a mass-radius relationship). There is, however, a handful of local white dwarfs with spectroscopically determined masses near this value (cf. Table 1 in [214]), which allows the construction of a semi-empirical cooling sequence for $M_{\text{WD}}=0.53 M_{\odot}$, once relatively small mass-dependent corrections are applied to each local white dwarf.

However, there are also some systematic differences between clusters ([180]): At a given metallicity some globular clusters (e.g. NGC 6752) possess very blue horizontal branches with horizontal branch star masses as low as $0.50 M_{\odot}$. Such extreme horizontal branch stars evolve directly to low-mass C/O-core white dwarfs (bypassing the asymptotic giant branch, therefore also called AGB-manqué stars, [81]) and shift the mean white dwarf mass closer to $0.51 M_{\odot}$. Other clusters show only very red horizontal branch stars, which will evolve along the asymptotic giant branch (thermal pulsing AGB) and form preferably white dwarfs with masses of about $0.55 M_{\odot}$, depending on the mass-loss efficiency along the asymptotic giant branch.

Also other channels may exist to produce white dwarfs with masses above or below the cluster mean, as described in Sect. 4.1. The spectroscopic determination of the white dwarf masses in a globular cluster was first attempted by [145] for white dwarfs in NGC 6397. However, the low S/N ratio of the spectra of these very faint stars did not allow them to determine the mass with sufficient accuracy. Multi-colour photometry of white dwarfs in NGC 6752 in combination with low-resolution spectra allowed [148] to estimate a most probable mass of $0.53 M_{\odot}$ for the bright white dwarfs in this cluster (assuming a true distance modulus of $(m - M)_0 = 13.20$ and a hydrogen layer mass of $10^{-4} M_{\odot}$).

Using spectroscopy of six white dwarf members of M 4 to fit effective temperatures and surface gravities [115] derive masses via the mass-radius relation. The masses are adjusted by $+0.034 M_{\odot}$ as suggested by the model spectra of [198] and yield an average mass of $0.53 \pm 0.01 M_{\odot}$ in good agreement with theoretical expectations.

- *The white dwarf envelope mass*

In the case of DA white dwarfs the cooling sequence location depends also on the mass of the residual H-rich envelope. The thickness of the envelope is important for the energy loss rate of the white dwarf cores and also affects the white dwarf radius at a given temperature ([180]). For ranges in envelope mass from $10^{-4} M_{\odot}$ to $10^{-6} M_{\odot}$ the cooling sequences for DA white dwarfs differ by about 0.07 in M_V , whereas non-DA white dwarfs

show no difference. This also affects *spectroscopically* derived masses (see above), with the resulting mass being about $0.04 M_{\odot}$ higher when using the *evolutionary* envelope mass ($10^{-4} M_{\odot}$, [74]) as opposed to virtually zero envelope mass. This mass uncertainty corresponds to an uncertainty of 0.1 mag in the distance modulus and 1–1.5 Gyr in the age derived from the main sequence turnoff.

- *Spectral type*

DB stars are fainter than DA stars at a given colour, with the offset depending on the filter combination (i.e. the offset is greater in V vs. $B - V$ than in I vs. $V - I$). In the field we find a ratio of DA:non-DA of about 4:1 ([180], [197]), while the number for globular clusters appears to be much lower (cf. Sect. 3). As non-DAs have colour-magnitude relations different from DAs (DA white dwarfs are, at fixed luminosity, systematically cooler than DBs) their undetected presence in the white dwarf cooling sequence can bias the distance determination. Since the cooling sequences are well separated (e.g. in $B - V$) this effect can be accounted for by a prudent choice of filters. However, the possible occurrence of He-core white dwarfs makes the photometric identification of DA and DB white dwarfs a risky approach, since He-core white dwarfs, at fixed luminosity, are also systematically cooler than DB C/O core white dwarfs.

- *Chemical composition of the core (varying C/O profiles, He-core white dwarfs)*

While the structure of the C/O-core is not well known, even large changes do not significantly affect the position of the cooling sequence ([180]). He-core white dwarfs are, at fixed mass and effective temperature, brighter than C/O-core white dwarfs, but their cooling sequences can overlap in the $M_V, V - I$ plane.

- *Initial-to-final mass relation*

For the initial-to-final mass relation assumed by [180] white dwarfs with progenitor masses below $2.5 M_{\odot}$ have a mass of $0.54 M_{\odot}$, which increases to $1.0 M_{\odot}$ for progenitor masses of $7 M_{\odot}$. Regardless of the assumed initial-to-final mass relation the masses of the white dwarfs are constant for the temperature range between 10,000 K and 20,000 K (although the actual value varies with the adopted initial-to-final mass relation). Also the progenitor masses are basically constant for this temperature range, since the white dwarf evolution is very fast when compared to the cluster ages. This is not true for the *field* stars, where due to extended star formation white dwarfs of different ages and masses can occupy a given temperature range. Using masses for white dwarfs in M4 as well as for white dwarfs in various open clusters [115] derive a linear initial-final-mass relation with no dependency on metallicity.

- *Reddening*

An uncertainty of 0.01 mag in E_{B-V} yields an uncertainty of 0.055 mag in the true distance modulus ([180]).

The first determination of the distance to a globular cluster using its white dwarf sequence was provided by [168] using WFPC2 data. Their distance modulus for NGC 6752 of $(m - M)_0 = 13.05 \pm 0.1$ was a bit lower than, but consistent with, the ones obtained from main sequence fitting ($13.12 \div 13.23$, see [148] for a discussion). In 2001 [214] repeated this experiment for 47 Tuc, again using WFPC2. The brightnesses of the local white dwarfs were corrected to a mass of $0.53 M_\odot$ assuming a hydrogen envelope mass of $10^{-4} M_\odot$. They obtained a true distance modulus of $(m - M)_0 = 13.09 \pm 0.14$, which was significantly shorter than all previously determined distances for 47 Tuc. Using the new value for the hydrogen layer mass they also provided a new white dwarf distance of $(m - M)_V = 13.27$ to NGC 6752. Shortly afterward [160] re-determined the distance to 47 Tuc from main-sequence fitting, noting possible calibration problems with previous studies. They found a best-fit value of $(m - M)_0 = 13.25^{+0.06}_{-0.07}$, which is in good agreement with the distance derived from the red clump $(m - M)_0 = 13.31 \pm 0.05$ and (within the mutual error bars) with the white dwarf distance derived by [214].

In 2004 [148] used FORS1 spectroscopy of white dwarfs in NGC 6397 and NGC 6752 to estimate a distance modulus to NGC 6397. The average gravity obtained from multi-colour WFPC2 photometry for the white dwarfs in NGC 6752 (assuming a fixed distance modulus) was used to determine effective temperatures from the spectra for the white dwarfs in NGC 6397. Using the effective temperatures determined that way to estimate the distance of the cluster yielded a true distance modulus of $(m - M)_0 = 12.0 \pm 0.1$, which is at the short end of the range of distances derived for NGC 6397 from main-sequence fitting ($12.1 \div 12.2$, [164, 165]). This result is in agreement with the one obtained by [89] ($(m - M)_0 = 12.02 \pm 0.06$) from deep ACS photometry (down to $m_{F814W} = 28$) of NGC 6397 (see below for the age derived from these data).

Using WFPC2 data [132] determined the distance to M5 from both the main sequence ($(m - M)_V = 14.56 \pm 0.10$, consistent with previous determinations) and the white dwarf sequence ($(m - M)_V = 14.78 \pm 0.18$). They ascribe the rather large error of their white dwarf distance to the low S/N of the observed white dwarfs, the small baseline in colour ($V - I$), and the mediocre spatial resolution of their WFPC2 data. These arguments should be considered in further attempts to determine white dwarf distances to globular clusters.

In a recent investigation [30] showed that the relative distances between ω Cen and 47 Tuc based on different distance indicators (tip of the RGB [TRGB], RR Lyrae, cluster kinematic) agree within one σ . However, absolute kinematic distance moduli are 0.2–0.3 mag smaller than distances based on the other methods. The same outcome apply to the distances to 47 Tuc based on the white dwarf cooling sequence and on the zero age horizontal branch — they agree within 0.1 mag, but they are on average 0.1–0.3 mag smaller than the distances based on the TRGB and on the RR Lyrae.

5.2 Cluster Age Determinations

The white dwarf sequence also provides a possibility to determine the age of a globular cluster. However, aside from the observational difficulties and the uncertainties in the cooling tracks (see [45] for more details) any error in the assumed mass affects the result. Very deep WFPC2 observations allowed [173] to detect the white dwarf cooling sequence in M 4 to unprecedented depths of $V \approx 30$. As a preliminary result [83] derived an age of 12.7 ± 0.7 Gyr from the white dwarf luminosity function of M 4, where the cluster membership of the stars had been verified from proper motions. This age is consistent with other independent age estimates, but one should keep in mind that their error bar does not include errors due to the uncertainty of the white dwarf mass. Their result had been questioned by [58], who claimed that the cluster membership of the white dwarfs cannot be verified down to sufficiently faint limits to obtain more than a lower limit of the age. In response to that claim [175] argued that with different methods for data reduction and analysis different limiting magnitudes can be reached using the same data.

In a more detailed paper [87] carefully studied the influence of the following parameters on the age determination: distance, reddening, atmospheric models, cooling models, main sequence lifetime, initial-to-final mass relation, core composition, atmospheric composition, and binary fraction.

To determine the age they performed a 2-dimensional modeling of the white dwarf cooling sequence, i.e. they modeled magnitude *and* colour. They started from a main sequence initial mass function (IMF), using an initial-to-final mass relation, and then assigned colour and magnitude based on the white dwarf cooling age. This way they derived an age of $12.4_{-1.5}^{+1.8}$ Gyr (2σ limits) for an IMF slope ($dN/dM_{ms} \sim M_{ms}^{-(1+x)}$) of $x = -0.85$. Variations of the input parameters envelope mass, C/O ratio in the core, initial mass function, cooling models, atmospheric composition (H-rich vs. He-rich), atmospheric models, binary fraction, proper motion cutoff, and distance yielded a global best fit for an age of 12.1 Gyr and an IMF slope of $x = -1.2$ with a 2σ lower age limit of 10.3 Gyr, in good agreement with other determinations, but with substantially larger uncertainties than their preliminary result in [83]. IMF slope and age are correlated as larger ages require that a larger fraction of the white dwarfs has cooled to below the detection limit, so that a smaller value of x is required to fit the observed star counts. One should keep in mind that the x values derived by the fitting procedure are local ones (based on one region within the globular cluster) and may be influenced by the effects of mass segregation.

They estimated a current birth rate of white dwarfs of $1.5 \times 10^{-6} \text{ yr}^{-1}$, which is consistent with the birth rate of horizontal branch stars for that cluster.

In their analysis of ACS observations of M 4 [15] concentrate on the detection of the faintest objects. This was achieved by restricting the searches for those objects to areas with an as flat as possible background (e.g. far from

bright stars). This way they reach $m_{F606W} = 28.95$ (50% completeness) in about 20% of the covered area (compared to 26.92 for the full region). The method is verified with similar data on NGC 6397. In the deep areas they reach the end of the white dwarf cooling sequence in M 4, from which they derive an age of 11.6 ± 0.6 Gyr (internal errors only). This is consistent with the age of 12.0 ± 1.4 Gyr derived from the main sequence turnoff. This paper as well as [87] are critically discussed by [115], who point out various uncertainties not addressed in the original papers.

According to [177] the peak in the white dwarf luminosity function is expected to move by about 1 mag/Gyr for ages of 12–14 Gyr, providing a very sensitive age indicator if the white dwarf cooling sequence is caught completely.

Using deep ACS photometry (down to $m_{F814W} = 28$) of NGC 6397 [89] derived age, reddening, distance, and an initial-to-final mass relationship from a fit of the complete white dwarf sequence (magnitude *and* colour, similar to their work on M 4 [87]). Using various evolutionary sequences they arrived at an age of 11.47 ± 0.47 Gyr (95% confidence limits) in agreement with, but more precise than, previous determinations from the main sequence turnoff. All models, however, fail to reproduce the full extent of the blueward turn at the faint end of the observed white dwarf cooling sequence. The initial-to-final mass relation which they derived simultaneously from their data is in good agreement with the empirical one from [208] and also with the white dwarf mass estimated at the bright end by [148].

On the theoretical side, [159] addressed the uncertainties affecting cluster age determinations based on the white dwarf luminosity function. In particular, they found that different assumptions concerning the conductive opacities might affect the ages of globular clusters at the 10% level, while the impact of the C/O ratio in the core is smaller than 5%. Interestingly enough, they also found that the cluster age is only marginally affected by the adopted initial mass function, since it does not affect the position of the peak in the luminosity function. On the other hand, the adopted initial-to-final mass relation affects both the shape and the position of the peak of the luminosity function. The change causes an uncertainty on the cluster age of about 8%. A similar uncertainty on the cluster age is also caused by the metal abundance, and indeed for progenitors with metallicities ranging from $Z=0.0001$ to $Z=0.001$ and from $Z=0.001$ to $Z=0.006$ the difference is of the order of 10% on average (see also [181] and [158]).

In a recent investigation [129] included Ly_α red wing opacity in the pure hydrogen white dwarf atmosphere models. He found that this physical ingredient plays a relevant role in the analysis of cluster white dwarf cooling sequences. The application of the new models to NGC 6397 suggests that the white dwarfs at the end of its cooling sequence are about 160 K cooler, and in turn that the cluster is about 0.5 Gyr older than previously estimated by [89].

6 Future Perspectives

While several recent photometric and spectroscopic investigations of cluster white dwarfs significantly improved our knowledge of these objects we are still facing longstanding problems. The right instruments to properly address these problems will be future extremely large telescopes like the European Extremely Large Telescope (E-ELT⁴, [99]; [28]), the Thirty Meter Telescope⁵, or the Giant Magellan Telescope⁶. The use of multi-conjugate adaptive optic systems ([141]) will provide near-infrared (NIR) images with a full width at half maximum (FWHM) of the order of a few hundredths of arc seconds, a field of view (FoV) of a few arcminutes squared and very high spatial resolution (from 0.005" to 0.01", see, e.g., [68]). The same outcome applies to the James Webb Space Telescope⁷. This telescope will be equipped with a NIR Camera (NIRCam⁸) covering the wavelength range from 0.6 to 5 μm with a FoV of $2.2 \times 4.4 \square'$ for simultaneous observations in two wavelength ranges. The short wavelength ($\lambda \leq 2.4 \mu\text{m}$) channels have a spatial sampling of 0.03"/px, while the long ones have 0.06"/px with Nyquist sampling at 2 and 4 μm ([178]). In addition the NIR spectrograph (NIRspec⁹) covers the same wavelength region at low spectral resolution ($R \approx 3000$). The key advantage of this choice is the possibility to collect spectra of faint targets located close to bright sources ([138]). This is a very typical situation in the crowded central regions of globular clusters. There are several fields where these observational equipments might play a crucial role.

i) Variable Stars – The 30m–40m class telescopes will provide the unique opportunity to collect multi-band photometry of globular cluster white dwarfs with an unprecedented time resolution. This means that we should be able to investigate *in situ* the topology of the instability strips located along the cooling sequence of cluster white dwarfs ([119]). Variable white dwarfs are multi-periodic non-radial oscillators with periods ranging from a few tenths to roughly 1000 seconds ([190]) and present small luminosity amplitudes. Starting at the hot end of the white dwarf cooling sequence we first find the instability strip of hot ($80,000 \text{ K} \leq T_{\text{eff}} \leq 170,000 \text{ K}$) either pre-white dwarfs or central stars of planetary nebulae. They are called DOV or GW Vir stars and the prototype is PG1159–035. The instability strip of DBV stars is located at cooler effective temperatures ($22,000 \text{ K} \leq T_{\text{eff}} \leq 28,000 \text{ K}$). Eventually, we approach the instability strip of the DAV or ZZ Ceti variables at even cooler effective temperatures ($11,000 \text{ K} \leq T_{\text{eff}} \leq 12,500 \text{ K}$). Note that the current knowledge on variable white dwarfs is based on local objects only, which are affected by uncertainties in the progenitor mix, the distance, the reddening,

⁴ <http://www.eso.org/projects/e-elt/>

⁵ <http://www.tmt.org/>

⁶ <http://www.gmto.org/>

⁷ <http://www.stsci.edu/jwst/>

⁸ <http://ircamera.as.arizona.edu/nircam/>

⁹ <http://sci.esa.int/science-e/www/object/index.cfm?fobjectid=456940>

and the effective temperature. Cluster variable white dwarfs will provide firm constraints on the driving mechanisms and the possible occurrence of static stars inside the various instability strips ([191]).

Moreover, the detection of cluster DBVs might provide fundamental constraints on plasmon neutrinos. The neutrino produced in the decay of plasmons cannot be observed in physics laboratories ([103]). However, current theoretical predictions indicate that half of the luminosity of a hot white dwarf ($T_{\text{eff}} \approx 25,000\text{ K}$) is carried away by neutrino emission ([152]; [120]). This means that accurate measurements of period changes over time for DBV stars can constrain plasmon neutrino rates ([211]). The great advantage of using cluster DBVs is the possibility to compare the plasmon neutrino rates based on pulsation observables with those based on evolutionary observables (white dwarf luminosity function). Current luminosity functions of white dwarfs in globular clusters do not provide firm constraints on this mechanism as the critical temperature range of the cooling sequence is too poorly populated.

Cluster white dwarf variables can also play an important role for even more fundamental physics. It has been suggested ([2]) that compact objects, such as neutron stars, might consist of Strange Quark Matter (**SQM**). SQM is a particular form of quark matter with a strangeness per baryon value of about -1 ([25]; [212]). Theoretical predictions indicate that SQM may also exist in the cores of white dwarfs ([79]; [202]). Two different observational approaches have been suggested to constrain the existence of exotic white dwarfs with SQM cores and envelopes of normal matter. *i*) The mass-radius relation. However, the difference between normal and exotic white dwarfs is too small to be observable (see Fig. 4 in [154]). *ii*) Gravity modes. Pulsations are very sensitive to density profiles and [19], [20], and [21] demonstrated that white dwarf models with SQM cores show a completely new resonant cavity for gravity modes. This causes the period spacing between consecutive modes in exotic white dwarfs to be shorter than one second, while in normal white dwarfs it is of the order of several tens of seconds. Moreover, the number of modes inside the different clusters of periods strongly depends on the size of the SQM core. The observational signature of this effect is that the Fourier spectrum of exotic white dwarfs should show peaks that are characterized by an intrinsic width, while those of normal white dwarfs become sharper with increasing time coverage. Cluster white dwarf variables will provide the large homogeneous samples required to constrain the possible occurrence of these phenomena.

Longer time series data covering several hours will also provide fundamental constraints on the number of cataclysmic variables in globular clusters as well as on the frequency of dwarf novae.

ii) Metals and IR Excess – White dwarfs have metal-poor atmospheres. Whatever the metal abundance of the progenitor, heavy elements in their atmosphere can only survive for a short period ($\approx 10^7$ yr). This empirical evidence is supported by the plain physical argument that radiative levitation is stronger than gravitational settling only at the hot end of the white

dwarf cooling sequence ($T_{\text{eff}} \geq 20,000 \text{ K}$, [46], and references therein). Cooler white dwarfs are characterized by diffusion timescales that are several orders of magnitude shorter than the cooling lifetime. Therefore, the occurrence of metal lines in the photospheres of cool white dwarfs must be due either to the inward growth of the convective region that dredges-up carbon ([69]) or to accretion of interstellar matter ([127]). Detailed theoretical calculations indicate that the diffusion timescale of Ca, Mg, and Fe in “metal-rich” DA (DAZ) white dwarfs are 3–4 orders of magnitude shorter than for “metal-rich” non-DA (DZ) white dwarfs (10^6 yr , [128]). This means that DAZ white dwarfs provide a unique opportunity to measure the actual accretion rate and to constrain small scale variations of the composition of the interstellar medium by comparing the composition of the white dwarfs (dominated by accretion while moving through the interstellar medium) to the local properties of the interstellar medium. The detection of cluster DAZ white dwarfs will provide the opportunity to measure the efficiency of pollution and in particular to probe the extent and composition of intra-cluster material. This questions becomes even more intriguing if one accounts for the fact that one scenario to explain the nature of the contaminating elements envisages the tidal disruption of an asteroid and an ensuing infrared excess ([108]). This working hypothesis is supported by the discovery of several systems in the field showing both metal lines and a well defined infrared excess during the last few years ([109]; [204]). Moreover, [189] and [174] suggest that the millisecond pulsar PSR B1620–26 in the globular cluster M4 is a triple system including a white dwarf and a third body with a mass value of the order of a few Jupiter masses. The detection of a planet in a globular cluster of intermediate metallicity is relevant not only for constraining planetary formation mechanisms but also to investigate their survival rate in old dense stellar systems. The possible occurrence of planets in globular clusters might also have an impact on the evolutionary properties of cluster stars. It has been suggested by [193] that the presence of planets could affect the evolution of the parent stars, and in turn the morphology of the horizontal branch and the presence of low-mass white dwarfs. The occurrence of infrared excess among white dwarfs is typically explained as the presence either of dust (disks, circumstellar envelope) or of a low-luminosity companion. Thanks to near- (2MASS¹⁰) and mid-IR (Spitzer¹¹) photometric surveys a sizable fraction of white dwarfs hosting both stellar and substellar (brown dwarfs) companions have been identified ([206]; [110]; [59], and references therein). The detection of cluster white dwarfs that show a well defined NIR excess can provide useful constraints on the current fraction of binary stars, but also on the evolutionary properties of brown dwarfs in metal-poor regimes. The current and the next generation of NIR adaptive optics systems at the 10m class telescopes will allow us to tackle this important experiment. The quality of the images (FWHM $\leq 0.1''$ in the K-band) and the

¹⁰ <http://irsa.ipac.caltech.edu/Missions/2mass.html>

¹¹ <http://sha.ipac.caltech.edu/applications/Spitzer/SHA/>

field of view (1'') provide the opportunity to perform accurate photometry for large samples in crowded cluster regions down to limiting magnitudes of $K \approx 21.5\text{--}22$ with exposure times of less than one hour ([29]).

iii) Spectral Classification – Thanks to its superb spatial resolution and its larger collecting area the 30m–40m class telescopes will allow us to observe spectra of much fainter white dwarfs than today. This will be essential to answer the question of the ratio DA:non-DA in globular clusters.

iv) Missing Physical Ingredients – The comparison between theory and observations is a fundamental step in constraining the plausibility and the accuracy of the physical assumptions adopted to construct stellar models. With respect to globular cluster white dwarfs we are still facing several open problems. The mismatch between the observed blueward turn of the white dwarf cooling sequence in NGC 6397 and synthetic colour-magnitude diagrams indicates that theory shows a smoother transition to bluer colours than is observed. A plausible culprit of this discrepancy might be an underestimate of the CIA from molecular hydrogen. This working hypothesis is supported by recent theoretical investigations suggesting that new DA white dwarfs atmosphere models accounting for the Ly_α red wing opacity are systematically redder than the old ones ([129]). One of the two anonymous referees properly noted that quantitative constraints on the currently adopted CIA have also significant impact on the predictions of planetary spectra.

Circumstantial empirical evidence indicates that globular clusters with extremely hot horizontal branch stars (hot helium flashers, cf. Sec. 4.2) present an excess of white dwarfs when compared with main sequence turnoff stars. It has been suggested that a fraction of He-core white dwarfs might account for current star counts. However, the number of globular clusters for which sufficiently accurate and deep data are available is quite limited and we still also lack firm constraints on the accuracy of cooling lifetimes in the high temperature range ([37]).

Summarizing the previous sections we feel quite confident that the coming years will provide ample material for new reviews on white dwarfs in globular clusters – and we look forward to reading them!

Acknowledgement. It is a pleasure to thank C.E. Corsi, G. Prada Moroni and M. Salaris for several useful discussions on white dwarfs, and H. Kuntschner for information on the instruments of the James Webb Space Telescope. This work was partially supported by ASI (P.I.: F. Ferraro) and by PRIN-MIUR 2009 (P.I. R. Gratton). One of us, G.B., acknowledges support from the ESO Visitor program. Extensive use has been made of both the ADS and the arXiv preprint archive. We also thank two anonymous referees for their suggestions and comments that helped to improve the quality of the manuscript.

References

1. M. D. Albrow, R. L. Gilliland, T. M. Brown, et al.: ApJ **559**, 1060 (2001)
2. C. Alcock, A. Olinto: Ann. Rev. Nuc. Part. Sci. **38**, 161 (1988)
3. L.G. Althaus, O. G. Benvenuto: MNRAS **296**, 206 (1998)
4. L. G. Althaus, A. H. Córsico, J. Isern, E. García Berro: A&ARv **18**, 471 (2010)
5. L. G. Althaus, E. García-Berro, I. Renedo, I. et al.: ApJ **719**, 612 (2010)
6. L. G. Althaus, J. A. Panei, A. D. Romero, et al.: A&A **502**, 207 (2009)
7. L. Angelini, M. Loewenstein, R. F. Mushotzky: ApJ **557**, L35 (2001)
8. C. G. Bassa, D. Pooley, L. Homer, et al.: ApJ **609**, 755 (2004)
9. H. Baumgardt, P. Hut, J. Makino, S. McMillan, S. Portegies Zwart: ApJ **582**, L21 (2003)
10. A. Beauchamp, F. Wesemael, P. Bergeron, J. Liebert, R. A. Saffer: The DB and DBA white dwarfs: epitomes of hydrogen-deficient stars, In: *Hydrogen-Deficient Stars*, ed. by C.S. Jeffery, U. Heber, ASPC **96** (Astronomical Society of the Pacific, San Francisco), pp. 295 (1996)
11. L.R. Bedin, G. Piotto, J. Anderson, et al.: ApJ **605**, L125 (2004)
12. L.R. Bedin, M. Salaris, G. Piotto, et al.: ApJ **624**, L45 (2005)
13. L.R. Bedin, I.R. King, A. Anderson, et al.: ApJ, **678**, 1279 (2008)
14. L. R. Bedin, M. Salaris, G. Piotto, et al.: ApJ **679**, L29 (2008)
15. L. R. Bedin, M. Salaris, G. Piotto, et al.: ApJ **697**, 965 (2009)
16. L. R. Bedin, M. Salaris, I. R. King, et al.: ApJ **708**, L32 (2010)
17. A. Bellini, L. R. Bedin, G. Piotto, et al.: A&A **513**, A50 (2010)
18. M.J. Benacquista: Living Review Relativity **9**, 2 (2006)
<http://relativity.livingreviews.org/>
19. O.G. Benvenuto: JPG **31**, L13 (2005)
20. O.G. Benvenuto: MNRAS **368**, 553 (2006)
21. O.G. Benvenuto: MNRAS **371**, 1351 (2006)
22. O. G. Benvenuto, L. G. Althaus: MNRAS **288**, 1004 (1997)
23. P. Bergeron, F. Wesemael, A. Beauchamp: PASP **107**, 1047 (1995)
24. L. Bildsten, D. M. Hall: ApJ **549**, L219 (2001)
25. A. R. Bodmer: Phys. Rev. D **4**, 1601 (1971)
26. G. Bono, F. Caputo, S. Cassisi, et al.: ApJ **543**, 955 (2000)
27. G. Bono, M. Monelli, P. B. Stetson, et al.: White dwarfs in ω Centauri: Preliminary Evidence, In: *14th European Workshop on White Dwarfs*, ed. by D. Koester, S. Moehler, ASPC **334** (Astronomical Society of the Pacific, San Francisco), 55 (2005)
28. G. Bono, S. Pedicelli, I. Ferraro, et al.: Accurate and Deep Wide Field Photometry: The Stellar Perspective In: *Large Astronomical Infrastructures at CONCORDIA, prospect and constraints for Antarctic Optical/IR Astronomy*, ed. by N. Epchtein, M. Candidi, EAS Publ.Series **25**, 125 (2007)
29. G. Bono, A. Calamida, C.E. Corsi, et al.: MAD@VLT: Deep into the Madding Crowd of ω Centauri In *Science with the VLT in the ELT era*, ed. by A. Moorwood, (Astrophysics and Space Science Proceedings, Springer: Netherlands), p. 67 (2009)
30. G. Bono, P. B. Stetson, N. Sanna, et al.: ApJ **686**, L87 (2008)
31. G. Bono, P. B. Stetson, D. VandenBerg, et al.: ApJ **708**, L74 (2010)
32. N. J. Brassington, G. Fabbiano, S. Blake, et al.: ApJ **725**, 1805 (2010)
33. E. Brocato, V. Castellani, M. Romaniello: A&A, **345**, 499 (1999)

34. T. M. Brown, A. V. Sweigart, T. Lanz, W. B. Landsman, I. Hubeny: ApJ
35. T. M. Brown, A. V. Sweigart, T. Lanz, et al.: ApJ **718**, 1332 (2010) **562**, 368 (2001)
36. G. Busso, G. Piotto, S. Cassisi, et al.: A&A **474**, 105
37. A. Calamida, C.E. Corsi, G. Bono, et al.: ApJ **673**, L29 (2008)
38. A. Calamida, C.E. Corsi, G. Bono, et al.: MmSAI **79**, 347 (2008)
39. V. Caloi, F. D'Antona: A&A **463**, 949 (2007)
40. S. Cassisi, M. Salaris, J. Anderson, et al.: ApJ **702**, 1530 (2009)
41. M. Castellani, V. Castellani: ApJ **407**, 649 (1993)
42. V. Castellani, V. Luridiana, M. Romaniello: ApJ, **428**, 633 (1994)
43. M. Castellani, V. Castellani, P. G. Prada Moroni: A&A **457**, 569 (2006)
44. V. Castellani, A. Calamida, G. Bono, et al.: ApJ **663**, 1021 (2007)
45. G. Chabrier, P. Brassard, G. Fontaine, D. Saumon: ApJ **543**, 216 (2000)
46. P. Chayer, G. Fontaine, F. Wesemael: ApJS **99**, 189 (1995)
47. G. W. Clark: ApJ **253**, L143 (1975)
48. H. N. Cohn, P. M. Lugger, S. M. Couch, et al.: ApJ **722**, 20 (2010)
49. A. M. Cool, G. Piotto, I. R. King: ApJ **468**, 655 (1996)
50. A. M. Cool, J. E. Grindlay, H. N. Cohn, P. M. Lugger, C. D. Bailyn: ApJ **508**, L75
51. F. D'Antona, I. Mazzitelli: ARA&A **28**, 139 (1990)
52. F. D'Antona, M. Bellazzini, F. Fusi Pecci, et al.: ApJ **631**, 868 (2005)
53. F. D'Antona, P. Ventura: MNRAS **379**, 1431
54. M. B. Davies: NewA **12**, 201 (2006)
55. D. S. Davis, H. B. Richer, I. R. King, et al.: MNRAS **383**, L20 (2008)
56. S. D. Davis, H. B. Richer, R. M. Rich, D. R. Reitzel, J. S. Kalirai: ApJ **705**, 398 (2009)
57. N. L. D'Cruz, B. Dorman, R. T. Rood: ApJ **466**, 359 (1996)
58. G. de Marchi, F. Paresce, F., O. Straniero, P. G. Prada Moroni: A&A **415**, 971 (2004)
59. J. H. Debes, S. Sigurdsson, B. Hansen: **134**, 1662 (2007)
60. C. J. Deloye, L. Bildsten: ApJ **580**, 1077 (2002)
61. A. Dieball, C. Knigge, D. R. Zurek, M. M. Shara, K.S. Long: ApJ **625**, 156 (2005)
62. A. Dieball, C. Knigge, D. R. Zurek et al.: ApJ **670**, 379 (2007)
63. A. Dieball, K.S. Long, C. Knigge, G. S. Thomson, D.R. Zurek: ApJ **710**, 332 (2010)
64. J. M. B. Downing, A. Sills: ApJ **662**, 341 (2007)
65. G.A. Drukier, H.N. Cohn, P.M. Lugger, H. Yong: ApJ **518**, 233 (1999)
66. P. D. Edmonds, J. E. Grindlay, A. Cool, et al.: ApJ **516**, 250 (1999)
67. R. A. W. Elson, G. F. Gilmore, B. X. Santiago, S. Casertano: AJ **110**, 682 (1995)
68. http://www.eso.org/projects/e-elt/Publications/ELT_INSWG_FINAL_REPORT.pdf
69. J. Farihi, B. Zuckerman, E. E. Becklin: ApJ **674**, 431 (2008)
70. M. Fellhauer, D. N. C. Lin, M. Bolte, S. J. Aarseth, K. A. Williams: ApJ **595**, L53 (2003)
71. F. R. Ferraro, N. D'Amico, A. Possenti, R. P. Mignani, B. Paltrinieri: ApJ **561**, 337 (2001)
72. J. M. Fregeau: Binary Stars and Globular Cluster Dynamics, In: IAUS 246, *Dynamical Evolution of Dense Stellar Systems*, ed. by E. Vesperini, p. 239 (2008)

73. J. M. Fregeau, F. A. Rasio: ApJ **658**, 1047 (2007)
74. G. Fontaine, F. Wesemael: A critical look at the question of thick vs. thin hydrogen and helium envelopes in white dwarfs, In: *White Dwarfs, Proc. of the 10th European Workshop on White Dwarfs*, ed. by J. Isern, M. Hernanz, E. Garcia-Berro, Astrophysics and Space Science Library Vol. **214** (Kluwer Academic Publishers: Dordrecht), p. 173
75. G. Fontaine, P. Bergeron, P. Brassard: Old Ultracool White Dwarfs as Cosmological Probes, In: *White Dwarfs: Cosmological and Galactic Probes*, ed. by E. M. Sion, S. Vennes, H. L. Shipman Astrophysics and Space Science Library Vol. **332** (Springer: Dordrecht), 3 (2005)
76. J. M. Fregeau, N. Ivanova, F. A. Rasio: ApJ **707**, 1533 (2009)
77. J. Gerssen, R. P. van der Marel, K. Gebhardt, P. Guhathakurta, R. C. Peterson, C. Pryor: AJ **124**, 327 (2002)
78. P. Gil-Pons, T. Suda, M. Y. Fujimoto, E. Garcia-Berro: A&A **433**, 1037 (2005)
79. N. K. Glendinning, Ch. Kettner, F. Weber: ApJ **450**, 253 (1995)
80. L. Girardi, G. Bertelli, A. Bressan, et al.: 2002, A&A **391**, 195 (2002)
81. L. Greggio, A. Renzini: ApJ **364**, 35 (1990)
82. J. E. Grindlay, F. Camilo, C. O. Heinke, et al.: ApJ **581**, 470 (2002)
83. B. M. S. Hansen, J. Brewer, G. G. Fahlmann, et al.: ApJ **574**, L155 (2002)
84. B. M. S. Hansen, V. Kalogera, F. A. Rasio: ApJ **586**, 1364 (2003)
85. B. M. S. Hansen, J. Liebert: ARA&A **41**, 465 (2003)
86. B. M. S. Hansen: PhR **399**, 1 (2004)
87. B. M. S. Hansen, H. B. Richer, G. G. Fahlman, et al.: ApJS **155**, 551 (2004)
88. B. M. S. Hansen: ApJ **635**, 522 (2005)
89. B. M. S. Hansen, J. Anderson, J. Brewer, et al.: ApJ **671** 380 (2007)
90. W. E. Harris: AJ **112**, 1487 (1996)
91. N. C. Haurberg, G. M. G. Lubell, H. N. Cohn, et al.: ApJ **722**, 158 (2010)
92. C. O. Heinke, J. E. Grindlay, P. M. Lugger, et al.: ApJ **598**, 502 (2003)
93. C. O. Heinke, J. E. Grindlay, P. D. Edmonds, et al.: ApJ **625**, 796 (2005)
94. J. Heyl: MNRAS **381**, L70 (2007)
95. J. Heyl: MNRAS **382**, 915 (2007)
96. J. Heyl: MNRAS **385**, 231 (2008)
97. J. Heyl, M. Penrice: MNRAS **397**, L79 (2009)
98. W. Hillebrandt, J. C. Niemeyer: ARA&A **38**, 191 (2000)
99. I. Hook, G. Dalton, R. Gilmozzi: Scientific requirements for a European ELT, SPIE **6267**, 69 (2006)
100. C. J. Horowitz, A. S. Schneider, D. K. Berry, PhRvL **104**, 1101 (2010)
101. J. R. Hurley, S. J. Aarseth, M. M. Shara: ApJ **665**, 707 (2007)
102. I. Jr. Iben, A. Renzini: ARA&A **21**, 271 (1983)
103. N. Itoh, H. Hayashi, A. Nishikawa, Y. Kohyama: ApJS **102**, 411 (1996)
104. N. Ivanova, K. Belczynski, J. M. Fregeau, F. A. Rasio: MNRAS **358**, 572 (2005)
105. N. Ivanova, C. O. Heinke, F. A. Rasio, et al.: MNRAS **372**, 1043 (2006)
106. N. Ivanova, S. Chaichenets, J. Fregeau, et al.: ApJ **717**, 948 (2010)
107. J. A. Irwin, T. Brink, J. N. Bregman, T. P. Roberts: ApJ **712**, L1 (2010)
108. M. Jura: ApJ **584**, L91 (2003)
109. M. Jura, J. Farihi, B. Zuckerman, E. E. Becklin: AJ **133**, 1927 (2007)
110. M. Jura, J. Farihi, B. Zuckerman: ApJ **663**, 1258 (2007)
111. J. S. Kalirai, H. B. Richer, D. Reitzel, et al.: ApJ **618**, L123 (2005)
112. J. S. Kalirai, H. B. Richer, B. M. S. Hansen, D. Reitzel, R. M. Rich: ApJ **618**, L129 (2005)

113. J. S. Kalirai, P. Bergeron, B. M. S. Hansen, D. Kelson, D. B. Reitzel, R. M. Rich, H. B. Richer: *ApJ*, 671, 748 (2007)
114. J. S. Kalirai, B. M. S. Hansen, D. D. Kelson, et al.: *ApJ* **676**, 594 (2008)
115. J. S. Kalirai, S. D. Davis, H. B. Richer, et al.: *ApJ* **705**, 408 (2009)
116. J. S. Kalirai, H. B. Richer: *RSPTA* **368**, 755 (2010)
117. J. Kaluzny, A. Udalski: *AcA* **42**, 29 (1992)
118. I. J. Katz: *Nature* **253**, 698 (1975)
119. A. Kim, D. E. Winget, M. H. Montgomery, S. O. Kepler: *MmSAI* **77**, 376 (2006)
120. A. Kim: PhD Thesis, University of Texas at Austin, Publication Number: AAT 3285959. Source: DAI-B 68/10 (2008)
121. E. Kim, D. Kim, G. Fabbiano et al.: *ApJ* **647**, 276 (2006)
122. R. Kippenhahn, K. Kohl, A. Weigert: *ZA* **66**, 58 (1967)
123. C. Knigge, D. R. Zurek, M. M. Shara, K.S. Long: *ApJ* **579**, 752 (2002)
124. C. Knigge, D. R. Zurek, M. M. Shara, K. S. Long, R. L. Gilliland: *ApJ* **599**, 1320 (2003)
125. C. Knigge, A. Dieball, J. Maíz Apellániz, et al.: *ApJ* **683**, 1006 (2008)
126. D. Koester, G. Chanmugam: *RPPh* **53**, 837 (1990)
127. D. Koester, K. Rollenhagen, R. Napiwotzki, et al.: 2005, *A&A* **432**, 025 (2005)
128. D. Koester, D. Wilken: *A&A* **453**, 1051 (2006)
129. P. M. Kowalski: *A&A* **474**, 491 (2007)
130. W. Landsman, J. Aparicio, P. Bergeron, et al.: *ApJ* **481**, L93 (1997)
131. W. B. Landsman, R. C. Bohlin, S. G. Neff et al.: *AJ* **116**, 789 (1998)
132. A. C. Layden, A. Sarajedini, T. von Hippel, A. Cool: *ApJ* **632**, 266 (2005)
133. Y.-W. Lee, S.-J. Han, S.-L. Han , et al.: *ApJ* **621**, L57, (2005)
134. J. Liebert, G. Fontaine, F. Wesemael: *MemSAI* **58**, 17 (1987)
135. J. Liebert, R. A. Saffer, E. M. Green: *AJ* **107**, 1408 (1994)
136. J. Liebert, P. Bergeron, J. B. Holberg: *ApJS* **156**, 47 (2005)
137. M. Limongi, A. Chieffi: *ApJ* **592**, 404 (2003)
138. D. Lobb, D. Robertson: *ESASP*, **621**, 69 (2006)
139. T. J. Maccarone, A. Kundu, S. E. Zepf, K. L. Rhode: *Nature* **445**, 183 (2007)
140. A. Maeder, G. Meynet: *ARA&A*, **38**, 143 (2000)
141. E. Marchetti, R. Brast, B. Delabre, et al.: MAD star oriented: laboratory results for ground layer and multi-conjugate adaptive optics, *SPIE* **6272**, 21 (2006)
142. T. R. Marsh, V. S. Dhillon, S. R. Duck: *MNRAS* **275**, 828 (1995)
143. J. G. Mengel, P. G. Gross: *Ap&SS* **41**, 407 (1976)
144. M. M. Miller Bertolami, L. G. Althaus, K. Ungraub, A. Weiss: *A&A* **491**, 253 (2008)
145. S. Moehler, U. Heber, R. Napiwotzki, D. Koester, A. Renzini: *A&A* **354**, L75 (2000)
146. S. Moehler, A. V. Sweigart, W. B. Landsman, S. Dreizler: *A&A* **395**, 37 (2002)
147. S. Moehler, A. V. Sweigart, W. B. Landsman, N. J. Hammer, S. Dreizler: *A&A* **415**, 313 (2004)
148. S. Moehler, D. Koester, M. Zoccali, et al.: *A&A* **420**, 515 (2004)
149. M. Monelli, C. E. Corsi, V. Castellani, et al.: *ApJ* **621**, L117 (2005)
150. J. E. Norris: *ApJ* **612**, L25 (2004)
151. K. Nomoto: *ApJ*, **277**, 791 (1984)
152. M. S. O'Brien, S. D. Kawaler: *ApJ* **539**, 372 (2000)
153. S. Ortolani, L. Rosino: *A&A* **185**, 102 (1987)

154. J. A. Panei, L. G. Althaus, O. G. Benvenuto: *A&A* **353**, 970 (2000)
155. F. Paresce, G. de Marchi, M. Romaniello: *ApJ* **440**, 216 (1995)
156. F. Paresce, G. de Marchi, R. Jędrzejewski: *ApJ* **442**, L57 (1995)
157. A. Pietrinferni, S. Cassisi, M. Salaris, F. Castelli: *ApJ* **642**, 797 (2006)
158. P. G. Prada Moroni, O. Straniero: *ApJ* **581**, 585 (2002)
159. P. G. Prada Moroni, O. Straniero: *A&A* **466**, 1043 (2007)
160. S. M. Percival, M. Salaris, F. van Wyk, D. Kilkeny: *ApJ* **573**, 174 (2002)
161. G. Piotto, L. R. Bedin, J. Anderson, et al.: *ApJ* **661**, L53 (2007)
162. A. J. T. Poelarends, F. Herwig, N. Langer, A. Heger: *ApJ* **675**, 614 (2008)
163. D. Pooley, W. H. G. Lewin, S. F. Anderson, et al.: *ApJ* **591**, L131 (2003)
164. I.N. Reid: *AJ* **116**, 2929 (1998)
165. I.N. Reid, J.E. Gizis: *AJ* **115**, 204 (1998)
166. I. Renedo, L. G. Althaus, M. M. Miller Bertolami, et al.: *ApJ* **717**, 183 (2010)
167. A. Renzini, F. Fusi Pecci: *ARA&A* **26**, 199 (1988)
168. A. Renzini, A. Bragaglia, F. R. Ferraro, et al.: *ApJ* **465**, L23 (1996)
169. H. B. Richer, G. G. Fahlmann: *ApJ* **325**, 218 (1988)
170. H. B. Richer, G. G. Fahlmann, R. A. Ibata, et al.: *ApJ* **451**, L17 (1995)
171. H. B. Richer, G. G. Fahlmann, R. A. Ibata, et al.: *ApJ* **484**, L741 (1997)
172. H. B. Richer, B. Hansen, M. Limongi, et al.: *ApJ* **529**, 318 (2000)
173. H. B. Richer, J. Brewer, G. G. Fahlmann, et al.: *ApJ* **574**, L151 (2002)
174. H. B. Richer, R. Ibata, G. G. Fahlman, M. Huber: *ApJ* **597**, L45 (2003)
175. H. B. Richer, J. Brewer, G. G. Fahlmann, et al.: *AJ* **127**, 2904 (2004)
176. H. B. Richer, A. Dotter, J. Hurley, et al.: *AJ* **135**, 2141 (2008)
177. H. B. Richer, A. Dotter, J. Hurley, et al.: *AJ* **135**, 2141 (2008)
178. M.J. Rieke, D. Kelly, S. Horner: *SPIE* **5904**, 1 (2005)
179. M. Salaris, I. Domínguez, E. García-Berro, et al.: *ApJ*, **486**, 413 (1997)
180. M. Salaris, S. Cassisi, E. García-Berro, J. Isern, S. Torres: *A&A* **371**, 921 (2001)
181. M. Salaris, E. García-Berro, M. Hernanz, J. Isern, D. Saumon: *ApJ*, **544**, 1036 (2000)
182. M. Salaris, S. Cassisi, A. Pietrinferni, P. M. Kowalski, J. Isern: *ApJ* **716**, 1241 (2010)
183. E. L. Sandquist, A. R. Martel: *ApJ* **654**, L65 (2007)
184. A. M. Serenelli, L. G. Althaus, R. D. Rohrmann, O. G. Benvenuto: *MNRAS* **337**, 1091 (2002)
185. M. M. Shara, S. Hinkley, D. R. Zurek, C. Knigge, H. E. Bond: *AJ* **128**, 2847 (2004)
186. M. M. Shara, S. Hinkley, D. R. Zurek: *ApJ* **634**, 1272 (2005)
187. M. M. Shara, J. R. Hurley: *ApJ* **646**, 464 (2006)
188. L. Siess: *A&A* **476**, 893 (2007)
189. S. Sigurdsson, H. B. Richer, B. M. S. Hansen, I. H. Stairs, S. E. Thorsett: *Science* **301**, 193 (2003)
190. R. Silvotti, G. Fontaine, M. Pavlov, T. R. Marsh, V. S. Dhillon, S. Littlefair: Search for p-mode Pulsations in DA White Dwarfs with VLT-ULTRACAM, In: *15th European Workshop on White Dwarfs*, ed. by R. Napiwotzki and R.B. Matthew, ASPC **372** (Astronomical Society of the Pacific, San Francisco), 593 (2007)
191. R. Silvotti, M. Pavlov, G. Fontaine, T. Marsh, V. Dhillon: *MmSAI* **77**, 486 (2006)

192. A. Sollima, G. Beccari, F. R. Ferraro, et al.: MNRAS **380**, 781 (2007)
193. N. Soker, A. Hershenhorn: MNRAS **381**, 334 (2007)
194. J. M. Taylor, J. E. Grindlay, P. D. Edmonds, A. Cool: ApJ **553**, L169 (2001)
195. R. R. Strickler, A. M. Cool, J. Anderson, et al.: ApJ **699**, 40 (2009)
196. A. Tornambé: MNRAS **206**, 867 (1984)
197. P.-E. Tremblay, P. Bergeron: ApJ **672**, 1144 (2008)
198. P.-E. Tremblay, P. Bergeron: ApJ **696**, 1755 (2008)
199. R. van den Bosch, T. de Zeeuw, K. Gebhardt, E. Noyola, G. van de Ven: ApJ **641**, 852 (2006)
200. H. M. van Horn, ApJ **151**, 227 (1968)
201. J. Th. van Loon, M. L. Boyer, I. McDonald, ApJ **680**, L49 (2008)
202. Yu. L. Vartanyan, A. K. Grigoryan, T. R. Sargsyan: Astrophys. **47**, 189 (2004)
203. F. Verbunt, W.H.G. Lewin: Globular Cluster X-ray Sources. In: *Compact Stellar X-ray Sources*, ed. by W. H. G. Lewin, M. van der Klis, Cambridge Astrophysics Series, No. **39** (Cambridge, Cambridge University Press), p. 341 (2006)
204. T. von Hippel, M. J. Kuchner, M. Kilic, et al: ApJ **662**, 544 (2007)
205. B. Voss, D. Koester, R. Napiwotzki, N. Christlieb, D. Reimers: A&A **470**, 1079 (2007)
206. S. Wachter, D. W. Hoard, K. H. Hansen, et al.: ApJ **586**, 1356 (2003)
207. S. Wanaajo, M. Tamamura, N. Itoh, et al.: ApJ **593**, 968 (2003)
208. V. Weidemann: A&A **363**, 647 (2000)
209. K. A. Williams, M. Bolte: AJ **133**, 1490 (2007)
210. D. E. Winget, S. O. Kepler, F. Campos, et al.: ApJ **693**, L6 (2009)
211. D. E. Winget, D. J. Sullivan, T. S. Metcalfe, S. D. Kawaler, M. H. Montgomery: ApJ **602**, L109 (2004)
212. E. Witten: Phys. Rev. D **30**, 272 (1984)
213. S. E. Woosley, A. Heger, T. A. Weaver: RvMP **74**, 1015 (2002)
214. M. Zoccali, A. Renzini, S. Ortolani, et al.: ApJ **553**, 733 (2001)